u^* = $\sqrt{(g_c\tau_1)/\rho}$ = friction velocity, ft./hr.
u = velocity, ft./hr.
V = u/u_a = velocity ratio, dimensionless
x = axial distance along tube, ft.
y = $r - r_1$ = distance from wall, ft.
y^+ = dimensionless wall distance, dimensionless

Greek Letters

ϵ_H = $k_e/\rho c_p$ = eddy diffusivity of heat, sq.ft./hr.
ϵ_M = eddy diffusivity of momentum, sq.ft./hr.
ν = kinematic viscosity, sq.ft./hr.
ρ = density, lb.-mass/cu. ft.
τ = shear, lb.-force/sq.ft.
ψ = ϵ_H/ϵ_M, dimensionless

Subscripts

a = average
c = transition between laminar and turbulent zones
L = laminar flow
m = on r denotes radius of maximum velocity; on t denotes velocity weighted mean temperature
q, t = designates variables in successive integrations
S = slug flow
u = unadjusted
1 = at wall

LITERATURE CITED

1. Martinelli, R. C., *Trans. Am. Soc. Mech. Engrs.*, **69**, 947 (1947).
2. Lyon, R. N., *Chem. Eng. Progr.*, **47**, 75 (1951).
3. ———, "Liquid-Metals Handbook," 2 ed., A.E.C. and Bureau of Ships, Navy Department (1952).
4. Lubarsky, B., and S. J. Kaufman, *Natl. Advisory Comm. Aeronaut., Tech. Note 3336* (1955).
5. Dwyer, O. E., and P. S. Tu, *Chem. Eng. Progr. Symposium Ser. No. 30*, **56**, 183 (1960).
6. Rothfus, R. R., J. E. Walker, and G. A. Whan, *A.I.Ch.E. Journal*, **4**, No. 2, 240 (1958).
7. Bailey, R. V., *Oak Ridge Natl. Lab. Rept. 521* (1950).
8. Isakoff, S. E., and T. B. Drew, "Proceedings of the General Discussion on Heat Transfer," p. 405, Institution of Mechanical Engineers, London, and American Society of Mechanical Engineers, New York (1951).
9. Brown, H. E., B. H. Amstead, and B. E. Short, *Trans. Am. Soc. Mech. Engrs.*, **79**, 279 (1957).
10. Perry, J. H., "Chemical Engineers' Handbook," 3 ed., p. 377, McGraw-Hill, New York (1950).
11. Dingee, D. A., W. B. Bell, J. W. Chastain, and S. L. Fawcett, *Battelle Mem. Inst., Rep. 1026*, Columbus, Ohio (1955).
12. LeTourneau, B. W., R. E. Grimble, and J. E. Zerbe, *Trans. Am. Soc. Mech. Engrs.*, **79**, 1751 (1957).
13. de Stordeur, A. N., *Trans. Am. Nuc. Soc.*, **1**, No. 2, 54 (1958).
14. Miller, Philip, J. J. Byrnes, and D. M. Benforado, *A.I.Ch.E. Journal*, **2**, No. 2, 226 (1956).
15. Grimble, R. E., W. H. Bell, and S. L. Fawcett, *AECD-3975*, Battelle Memorial Institute, Columbus, Ohio (1954).
16. Knudsen, J. G., and D. L. Katz, "Proceedings of the Midwest Conference on Fluid Dynamics," p. 175, 1st Conf., University of Illinois (1950).
17. Hartnett, J. P., and T. F. Irvine, Jr., *A.I.Ch.E. Journal*, **3**, 313 (1957).

Manuscript received December 10, 1959; revision received May 13, 1960; paper accepted May 18, 1960.

Use of Boundary-Layer Theory to Predict the Effect of Heat Transfer on the Laminar-Flow Field in a Vertical Tube with a Constant-Temperature Wall

EDWARD M. ROSEN and THOMAS J. HANRATTY

University of Illinois, Urbana, Illinois

Variations of density and viscosity with temperature cause distortions in the flow field and affect the rate of heat transfer to fluids in laminar flow in vertical tubes. The magnitude of these distortions is predicted through an approximate solution of the equations of motion and energy.

Variation of density and viscosity with temperature may cause distortions in the parabolic flow field and may affect the rate of heat transfer and the stability of flow of fluids at low Reynolds numbers in vertical tubes with a constant-temperature wall. An analytical expression for the temperature field and the rate of heat transfer to fluids in laminar flow with constant properties was obtained by Graetz (*2*). Sellars, Tribus, and Klein (*15*) extended the solution of Graetz and provided all the necessary eigenvalues and eigenfunctions to construct the infinite-series solution. Whiteman and Drake (*18*) showed how other velocity profiles affect the rate of heat transfer; Singh (*17*) and Millsaps and Pohlhausen (*9*) included axial conduction and viscous dissipation in the solution, and Schenk and Dumore (*13*) calculated the effect of wall resistance.

Distortions of the parabolic laminar velocity profile due to viscosity variation were discussed by Keevil and McAdams (*6*). Hanratty, Rosen, and Kabel (*5*) and Scheele, Rosen, and Hanratty (*12*) described visual experiments on the effect of heating and cooling water in a vertical tube where density variation (natural convection) was more important than viscosity variation. Under relatively mild conditions of heating and cooling, distortions were found sufficient to change the parabolic velocity profile to such an extent that the flows became turbulent at Reynolds numbers much lower than those for isothermal flow. The results showed two types of instabilities. For cooling in upflow, transition to turbulence is associated with the condition at which the velocity gradient at the wall becomes zero and a reversal of flow occurs. The instability develops rapidly in such cases. For heating in upflow it appears as if a length of pipe is required to allow the instabilities in the flow to grow. Instabilities may be observed downstream of the point where the velocity profile at the center becomes flat

Edward M. Rosen is with Monsanto Chemical Company, St. Louis, Missouri.

and are always observed downstream of the point where the center-line velocity drops to zero (inversion point). It is the purpose of this study to describe the extent and location of these distortions for fluids of variable density and viscosity during heating and cooling in a vertical tube with a constant-temperature wall.

EQUATIONS DESCRIBING THE PROBLEM

The problem may be formulated as follows. A long, vertical, straight tube of circular cross section has a fluid flowing through it isothermally at a constant rate in laminar flow. After the fluid passes through a calming section, the entrance effects are eliminated and fully developed laminar flow exists, the velocity profile being parabolic. The fluid is suddenly heated or cooled by a change in the outside-wall temperature. If the wall has a finite resistance, the temperature on the inside of the tube wall will vary with distance downstream. It is desired to find the resulting temperature and the velocity fields.

Although the bulk of the calculations were performed for tubes of zero wall resistance (constant-temperature wall), it was necessary to develop the case of *finite* wall resistance (constant ambient temperature) so that the theory might be compared with experiment.

The problem is further described:

1. Steady state exists.
2. There is symmetry about the z axis.
3. Flow is incompressible; ρ varies only in the gravity force term.
4. The only body force is gravity acting downward.
5. Flow is vertical upward. For flow downward the sign of the gravity term must be changed.
6. There is no axial flow of heat in the walls.
7. There are no heat sources in the fluid.
8. Heating due to viscous dissipation may be neglected in the energy equation.
9. ρ and $1/\mu$ are linear functions of temperature:

$$\rho = \rho_o [1 - \beta (t - t_o)]$$
$$\frac{1}{\mu} = \frac{1}{\mu_o} [1 + b (t - t_o)]$$

Other physical properties are constant.

The exact solution to the problem defined above is unknown. Lee, Nelson, Cherry, and Boelter (*7*) and Yamagata (*19*), who studied the effect of variable viscosity; Martinelli and Boelter (*8*), who studied the effect of variable density; and Pigford (*10*), who studied the effect of variable density and viscosity, made boundary-layer assumptions which simplified the equations of motion and energy considerably. These assumptions, discussed by Schlichting (*14*), are listed below:

1. $\partial p/\partial r = 0$; that is, dp/dz is a function of z alone.
2. $\partial^2 t/\partial z^2 << [1/r\ (\partial t/\partial r) + \partial^2 t/\partial r^2]$
3. $\partial^2 u/\partial z^2 << [1/r\ (\partial u/\partial r) + \partial^2 u/\partial r^2]$
4. $[\partial u/\partial z]\ [\partial \mu/\partial z]$ and $[\partial v/\partial z]\ [\partial \mu/\partial r]$ are small compared with the other terms in the equation of motion.

When heating does not cause inversion to take place near the start of the heat transfer section or when cooling does not cause the velocity gradient at the wall to go to zero quickly, these assumptions should be fairly good; however when the inversion point or the point where the velocity gradient at the wall becomes zero is close to the start of the heat transfer section (large $|N_{Gr}/N_{Re}|$), flows in the radial direction become large and the boundary-layer assumptions are probably poor.

When the boundary-layer assumptions are applied and the expressions for the functionality of density and viscosity with temperature are used, together with the dimensionless groups defined in the notation, the equations defining the system assume the following form:

Equation of Continuity

$$\frac{\partial V^*}{\partial R} + \frac{V^*}{R} + \frac{\partial U}{\partial Z^*} = 0 \qquad (1)$$

Equation of Motion in the Z* Direction

$$V^* \frac{\partial U}{\partial R} + U \frac{\partial U}{\partial Z^*} = -\frac{dP}{\partial Z^*} - \pi N_{Pr} \frac{N_{Gr}}{N_{Re}} \left[\frac{T - 1}{1 - T_d} \right] + \pi N_{Pr} \frac{1}{R} \frac{\partial}{\partial R} \left[\frac{R \left(\frac{\partial U}{\partial R} \right)}{1 - \frac{\psi (T - 1)}{1 - T_d}} \right] \qquad (2)$$

Energy Equation

$$V^* \frac{\partial T}{\partial R} + U \frac{\partial T}{\partial Z^*} + \frac{U(T - 1)}{1 - T_d} \frac{dT_d}{dZ^*} = \pi \left[\frac{\partial^2 T}{\partial R^2} + \frac{1}{R} \frac{\partial T}{\partial R} \right] \qquad (3)$$

with boundary conditions:

$$T = 0 \quad \text{at } R = 1 \quad \text{for } Z^* > 0 \qquad (4)$$

$$\frac{1}{\lambda} \left[\frac{\partial T}{\partial R} \right]_{R=1} = T_d \quad \text{for } Z^* > 0 \qquad (5)$$

$$T = 1 \text{ at } Z^* = 0 \text{ for } 1 > R \geq 0 \qquad (6)$$

$$U = 2(1 - R^2) \text{ at all } R \text{ for } Z^* \leq 0 \qquad (7)$$

$$U = 0 \quad \text{at } R = 1 \quad \text{for all } Z^* \qquad (8)$$

All physical properties are evaluated at the entrance temperature, and it will be noted that the density was allowed to vary only in the gravity term. Boundary condition (5), which is deduced by writing a heat balance through the wall, introduces the wall resistance into the problem. Both the viscosity ratio parameter and the Grashof number are defined in terms of $(t_d - t_o)$, which is positive for heating and negative for cooling. For a wall of zero resistance $\lambda \to \infty$, $t_d \to t_w$, and $T_d \to 0$.

Several over-all integral relationships can now be derived. Equations (1), (2), and (3) may be integrated over the tube cross section to obtain a mass, momentum, and over-all energy balance respectively. In addition by multiplying the equation of motion in the Z^* direction by U and then integrating over the tube cross section, one can obtain a mechanical energy balance. Details of the integrations are given by Rosen (*11*). The results are

Mass Balance

$$\int_o^1 RU dR = \frac{1}{2} \qquad (9)$$

Momentum Balance

$$-\frac{dP}{dZ^*} = 2 \frac{d}{dZ^*} \int_o^1 RU^2 dR + \frac{\pi N_{Pr} N_{Gr}}{N_{Re}(1 - T_d)} (T_{avg} - 1) - \frac{2\pi N_{Pr} \left[\frac{\partial U}{\partial R} \right]_{R=1}}{\left[1 + \frac{\psi}{1 - T_d} \right]} \qquad (10)$$

Over-all Energy Balance

$$\frac{(T_m - 1)}{2(1 - T_d)} \frac{dT_d}{dZ^*} + \frac{d}{dZ^*} \int_o^1 RUT\, dR = \pi \left[\frac{\partial T}{\partial R} \right]_{R=1} \qquad (11)$$

Mechanical Energy Balance

$$-\frac{dP}{dZ^*} = \frac{d}{dZ^*} \int_o^1 RU^3 dR + \frac{\pi N_{Pr} N_{Gr}}{N_{Re}} \left[\frac{T_m - 1}{1 - T_d} \right] + 2\pi N_{Pr} \int_o^1 \frac{R \left[\frac{\partial U}{\partial R} \right]^2 dR}{\left[1 - \frac{\psi (T - 1)}{(1 - T_d)} \right]} \qquad (12)$$

where the dimensionless mean (mixing cup) and average temperatures are defined as

$$T_m = 2 \int_o^1 RUT dR \qquad (13)$$

and

$$T_{avg} = 2 \int_o^1 RT dR \qquad (14)$$

The system parameters are ψ, N_{Pr}, N_{Gr}/N_{Re}, and λ. The pressure gradient may be deduced from either Equation (10) or (12). It will be noted that the analysis for external flows given by Acrivos (*1*) leads to the parameter $N_{Gr}/(N_{Re})^2$. This is due to the fact that the pressure drop for external flows may be deduced from the flow far from the wall.

PREVIOUS APPROACHES

Heating in Upflow with Variable Density

Since the equations of motion and energy could not be solved simultaneously, Pigford (*10*), who combined the approaches of previous investigators (*7, 8,*

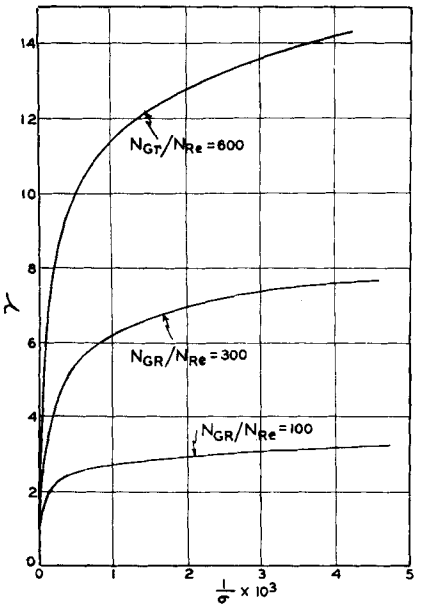

Fig. 1. Values of γ according to the solution of Pigford for heating in upflow with variable density.

19), solved the equation of motion independently of the energy equation. This was accomplished by considering the solution for $N_{Pr} \to \infty$ which simplifies Equation (2) (for $T_a \to O$) to

$$O = N_{Re}\frac{dP}{dZ} - \frac{N_{Gr}}{N_{Re}}(T\text{-}1) + \frac{1}{R}\frac{\partial}{\partial R}\left[\frac{R\left(\frac{\partial U}{\partial R}\right)}{1-\psi(T-1)}\right] \quad (15)$$

Equation (15) was integrated twice to give an expression for the velocity, and the pressure gradient was deduced from a mass balance. For the constant-viscosity case ($\psi = O$) the results are

$$U = 2(1\text{-}R^2) + \frac{N_{Gr}}{N_{Re}}\left[(2T_1\text{-}I_3)\frac{(1\text{-}R^4)}{4} + I_5\right] \quad (16)$$

$$-N_{Re}\frac{dP}{dZ} = 8 + \frac{N_{Gr}}{N_{Re}}[2T_1\text{-}I_3\text{-}1] \quad (17)$$

$$\gamma = 1 + \frac{N_{Gr}}{8N_{Re}}[I_1\text{-}I_3] \quad (18)$$

where

$$I_1(\sigma) = 2\int_0^1 RTdR = T_{avg} \quad (19)$$

$$I_3(\sigma) = 4\int_0^1 R^3TdR \quad (20)$$

$$I_5(R,\sigma) = \int_1^R \frac{1}{R}\left[\int_0^R RTdR\right]dR \quad (21)$$

and

$$\gamma = -\frac{1}{4}\left(\frac{\partial U}{\partial R}\right)_{R=1} \quad (22)$$

It was assumed the temperature field could be described by Leveque's solution of the energy equation (*8*), which is

$$T = \frac{1}{\Gamma(4/3)}\int_0^w e^{-w^3}dw \quad (23)$$

where

$$w = \left(\frac{\sigma}{9}\right)^{1/3}(1\text{-}R) \quad (24)$$

and

$$\sigma = \frac{4}{\pi}\gamma_{avg}N_{Gz} = \frac{4\gamma_{avg}}{\pi Z^*} \quad (25)$$

Pigford did not calculate the change in the velocity field as a function of the distance downstream, as he was interested only in deducing an average slope of the velocity profile at the wall (γ_{avg}), so that heat transfer coefficients might be calculated from a modified Leveque type of expression for the flux at the wall. (See notation.)

Use of the Leveque solution for the temperature field imposes several restrictions on the validity of the velocity profiles calculated from Equation (16). First, the Leveque solution was derived for the case of a constant velocity gradient at the wall. It was assumed that it could be used to represent temperature fields in which the velocity gradient at the wall is changing by introducing an average slope, γ_{avg}. Second, the Leveque solution was derived for a flat plate and not a tube and so would be applicable only very near the start of the heat transfer section. Third, although the velocity profile may be approximated by a straight line near the wall for heating, it becomes a poor approximation in cooling for situations in which the velocity gradient at the wall approaches zero (separation point).

With these restrictions in mind the integrals of Equations (19), (20), and (21) may be evaluated by means of Equation (23). The integrals $I_1(\sigma)$ and $I_3(\sigma)$ are given by Pigford (*10*), and $I_5(R, \sigma)$ is tabulated by Rosen (*11*). Figure 1 is a plot of γ vs. $1/\sigma$ at representative values of N_{Gr}/N_{Re} calculated from Equation (*18*), and Figure 2 shows the complete velocity profiles for $N_{Gr}/N_{Re} = 600$ calculated from Equation (16).

Before a value of Z^* can be associated with a value of σ, it is necessary to select a value for γ_{avg}. Martinelli and Boelter (*8*) used an integrated average value of γ; Pigford (*10*) however simply evaluated γ_{avg} at a point halfway down the tube. His procedure was

1. Select 2σ.
2. Compute γ_{avg} from Equation (18) at 2σ.
3. Compute Z^* from Equation (25) at σ.

In order to study the effect of evaluating γ_{avg} at σ's other than 2σ, γ_{avg} was evaluated at $\sigma = \infty$ (the start of the heat transfer section where $\gamma = 1$) and at $\sigma = \sigma$. At given values of N_{Gr}/N_{Re} the center-line velocity was then calculated from Equations (16) and (25) as a function of Z^* and plotted. From this plot the value of Z^* at which the center-line velocity became equal to zero was determined [values of $(Z^*)_{null}$]. These values are plotted in Figure 9.

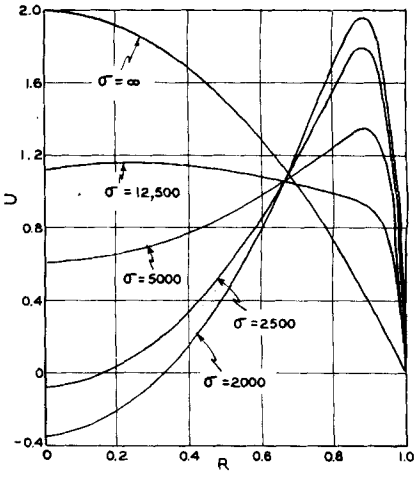

Fig. 2. Velocity profiles according to the solution of Pigford for heating in upflow with variable density for $N_{Gr}/N_{Re} = 600$.

Heating in Upflow with Variable Viscosity

Following the same procedures and utilizing the same assumptions as for the variable density case, one may integrate Equation (15) for negligible natural convection effects ($N_{Gr}/N_{Re} = O$) to give

$$U = \frac{2}{1+\psi(1\text{-}I_3)}[(1\text{-}R^2)(1+\psi) - 2\psi I_7] \quad (26)$$

$$-N_{Re}\frac{dP}{dZ} = \frac{8}{1+\psi(1\text{-}I_3)} \quad (27)$$

$$\gamma = \frac{1+\psi}{1+\psi(1\text{-}I_3)} \quad (28)$$

where

$$I_7(R,\sigma) = \int_R^1 RTdR \quad (29)$$

Equation (26) is equivalent to Yamagata's equation (183), and the function $I_7(R, \sigma)$ is tabulated by Rosen (*11*). Figure 3 shows the values of γ computed from Equation (28), and Figure 4 shows complete velocity profiles as a function of σ as computed from Equation (26).

ANALYSIS

In order to overcome some of the weaknesses of the Pigford solution another approach to the solution of the equations of motion and energy was attempted. This approach utilizes the same boundary-layer assumptions used by Pigford but solves the equations of motion and energy simultaneously and in addition retains the inertia terms which do not drop out for a finite N_{Pr}. The solution can be expected to apply over the whole range of Z^* rather than only to short tubes. It is valid for cooling in upflow as well as for heating.

The solution however is an approximate one and is intended only to describe the over-all flow characteristics of the field rather than its details. As a result it will be found that it satisfactorily predicts experimental inversion points but is rather poor in predicting heat transfer rates, since a detailed knowledge of the velocity field is necessary to do this accurately. The procedure is as follows. Equations in R are assumed for the velocity and temperature profiles with coefficients which are a function of Z^* alone. The general equations developed previously may then be used to impose conditions on these profiles. Substituting the approximate temperature and velocity profiles into these equations leads to a series of ordinary differential equations with the coefficients as dependent variables which are solved numerically for their dependence on Z^*. A discussion of the general methods and procedures utilizing this technique may be found in Schlichting (*14*).

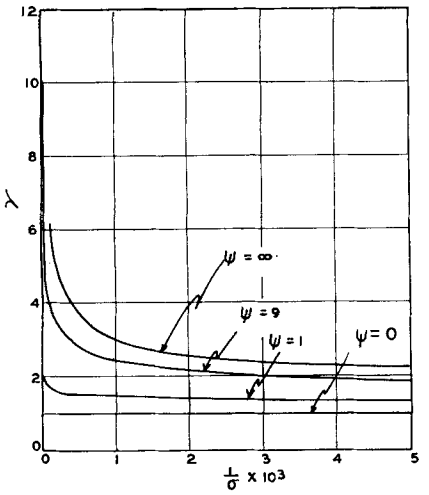

Fig. 3. Values of γ according to the solution of Pigford for heating in upflow with variable viscosity.

The nature of the assumed series for the profiles is governed by two criteria. The first is that the profile must be capable of representing the type of profiles which are expected to occur in the flow treated; the second is that there must be at least the same number of conditions imposed on the profiles as there are undetermined coefficients.

A direct numerical solution of the partial differential equations by the use of a finite difference scheme might be no more complicated than the method of moments used in this study. Integral methods are generally useful when one is able to reduce the original system of partial differential equations to no more than two or three ordinary differential equations. This approach however was not attempted by the authors.

Velocity Profile. Figures 2 and 4 as well as the constant-flux solutions of Hanratty, Rosen, and Kabel (*5*) and Hallman (*4*) show qualitatively the type of velocity profiles that may be expected to occur. Since the velocity profile is a parabola at the start of the heat transfer section and must return to one far downstream, a power series in R^2 suggests itself:

$$U = k_1 + k_2R^2 + k_3R^4 + \dots \quad (30)$$

where the k's are a function of Z^* alone. When $k_1 = 2$ and $k_2 = -2$ and $k_3, \dots =$ zero, the profile is a parabola.

The number of terms used in the series depends upon the number of available equations which the profile can be made to obey; however, there are a few practical difficulties which arise. First the algebra becomes excessive as the number of equations is increased. Second, the final expression for the derivatives of the coefficients, dk_1/dZ^*, dk_2/dZ^* . . ., must have denominators which do not go to zero over the range of integration, since the differential equations must be solved numerically.

The boundary conditions and possible equations which the profile could reasonably be expected to satisfy may be listed: (I) velocity zero at the wall, (II) mass balance, (III) equation of motion at the center, (IV) mechanical energy balance, (V) momentum balance, (VI) equation of motion at the wall or any R, and (VII) higher moments of the equation of motion where Equation of motion at the center:

$$\left[U \frac{\partial U}{\partial Z^*} \right]_{R=0} = -\frac{dP}{dZ^*} - \frac{\pi N_{Gr} N_{Pr}}{N_{Re}} \left[\frac{T_c - 1}{1 - T_a} \right] + \pi N_{Pr} \frac{\left[\frac{1}{R} \frac{\partial}{\partial R} \left(R \frac{\partial U}{\partial R} \right) \right]_{R=0}}{\left[1 - \frac{\psi(T_c - 1)}{1 - T_a} \right]} \quad (31)$$

Since conditions I and II must be satisfied, the choice of additional conditions is dependent largely on the practical considerations mentioned above. If a three-term series is used, two additional conditions must be met: one to determine the pressure drop and the other to fix the variation of the remaining coefficient with Z^*. If a four-term series is used, three additional conditions must be met: one to determine the pressure drop and two to determine the variation of the two remaining coefficients with Z^*. If more terms are used, more conditions must be satisfied.

The simplest series and the one used in this study is a three-term series which utilizes the equation of motion at the center and the mechanical energy balance. Details of the factors which guided the selection of these conditions are given by Rosen (*11*). The pressure drop may be thought of as being determined by the equation of motion at the center, and the mechanical energy balance may be thought of as determining the variation of k_1 with Z^*.

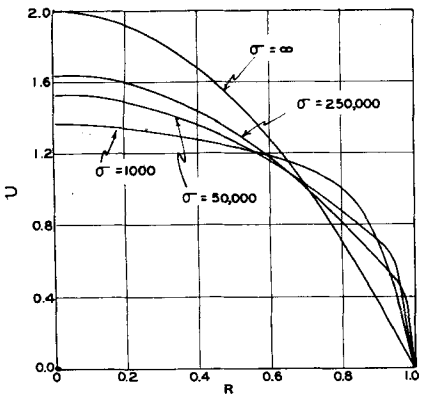

Fig. 4. Velocity profiles according to the solution of Pigford for heating in upflow with variable viscosity for $\psi = 9$.

Temperature Profile. In contrast to the velocity profile—which starts out as a parabola, is distorted by the heat transfer, and then returns to a parabola far downstream as the flow again becomes isothermal—the temperature profile starts out as a step function of height one and slowly decreases to a flat profile of zero height. Martinelli and Boelter (*8*) in fitting a curve to the Leveque temperature solution used an exponential series which they found to be satisfactory. Utilizing this form suggested the following series:

$$T = T_A T_c = T_c[C_1 + C_2e^{-K_3(1-R)/Z^{*1/3}} + C_3e^{-2K_3(1-R)/Z^{*1/3}} + C_4e^{-3K_3(1-R)/Z^{*1/3}} + C_5e^{-4K_3(1-R)/Z^{*1/3}} + \dots] \quad (32)$$

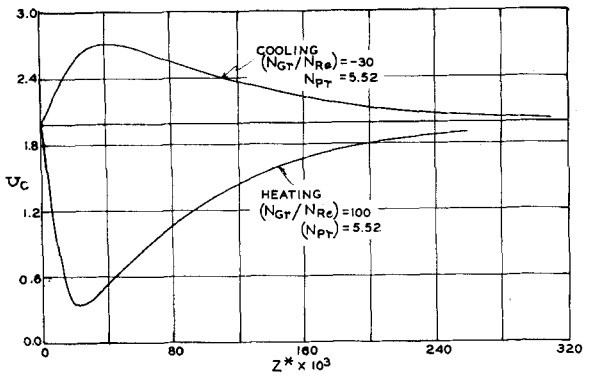

Fig. 5. Heating and cooling in upflow with variable density, changes in center-line velocity as a function of Z^*.

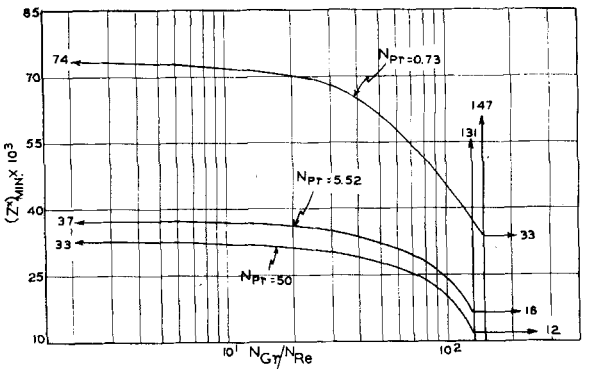

Fig. 7. Heating in upflow with variable density, values of $(Z^*)_{min}$

where the C's are a function of Z^* alone and K_8 is a constant.

In the same way as with the velocity profile, a number of conditions may be imposed on the temperature profile. Those which the profile may reasonably be expected to satisfy are (VIII) dimensionless temperature T, zero at the wall; (IX) energy balance through the wall; (X) slope at the center, zero; (XI) energy equation at the wall; (XII) energy equation at the center; (XIII) over-all energy balance; and (XIV) energy equation at any R, where

Slope at the center, zero:

$$\left[\frac{\partial T}{\partial R}\right]_{R=0} = 0 \qquad (33)$$

Energy equation at the wall:

$$\left[\frac{\partial^2 T}{\partial R^2} + \frac{1}{R}\frac{\partial T}{\partial R}\right]_{R=1} = 0 \quad (34)$$

Energy equation at the center:

$$\left[U\frac{\partial T}{\partial Z^*}\right]_{R=0} + \frac{U_c(T_c - 1)}{1 - T_a}\frac{dT_a}{dZ^*} = \pi\left[\frac{\partial^2 T}{\partial R^2} + \frac{1}{R}\frac{\partial T}{\partial R}\right]_{R=0} \quad (35)$$

Boundary conditions VIII and IX and condition X must be satisfied. The choice of additional conditions depends upon how many coefficients are desired. Unlike the velocity profile, however, a criterion is available which determines when a satisfactory number of coefficients have been selected. This criterion is the Graetz solution, which the approximate temperature profile should satisfy when the velocity profile remains a parabola and the wall temperature is a constant. First a four-coefficient series was tried but gave unsatisfactory agreement with the Graetz solution. Then a five-coefficient series was tried which utilized conditions X, XI, XII, and XIII. This approximated the Graetz solution satisfactorily (Figure 19). Attempts to improve the agreement by the use of six coefficients and condition XIV lead to excessive algebra and doubt as to the proper R at which to write the energy equation.

Development of the Approximate Differential Equations

The four independent conditions I, II, III, and IV define the pressure gradient and the three coefficients of the velocity profile; the six independent conditions VIII, IX, X, XI, XII, and XIII define the wall temperature function T_a and the five coefficients of the temperature profile. For convenience T_c was introduced into Equation (32), as it simplified some of the algebra and in addition acted as a scaling factor for the temperature profile. It was carried along as an additional dependent variable and introduced an additional equation from the definition of T_c at the center: (XV) $T_A = 1.0$ at $R = 0$.

The temperature and velocity profiles were substituted into the selected conditions and gave rise to two ordinary differential equations, two algebraic equations from the conditions on the velocity profile, and two ordinary differential equations and five algebraic equations from conditions on the temperature profile. L'Hospital's rule was used in the evaluation of the expression arising from condition XII.

If the pressure drop is now eliminated between the two equations arising from conditions III and IV, there remain a total of seven algebraic equations and three differential equations in the following ten unknown total differentials:

$$\frac{dk_1}{dZ^*}, \frac{dk_2}{dZ^*}, \frac{dk_3}{dZ^*}, \frac{dC_1}{dZ^*}, \frac{dC_2}{dZ^*}, \frac{dC_3}{dZ^*}, \frac{dC_4}{dZ^*}, \frac{dC_5}{dZ^*}, \frac{dT_c}{dZ^*}, \frac{dT_a}{dZ^*} \quad (36)$$

To set up the solution for these ten derivatives it is necessary to express each of them explicitly. First the seven algebraic expressions were converted to differential equations by differentiating them with respect to Z^*. The resulting ten equations in the ten unknown derivatives were then algebraically solved. The equations apply to the constant-temperature-wall case ($\lambda \to \infty$) as well as to the constant-ambient-temperature case (λ finite).

In order to begin the integration of the ten simultaneous nonlinear ordinary differential equations, it would be desirable to know the value of each of the ten dependent variables at $Z^* = 0$. Although the values of the k's are known (since the velocity profile is a parabola there) and the center-line

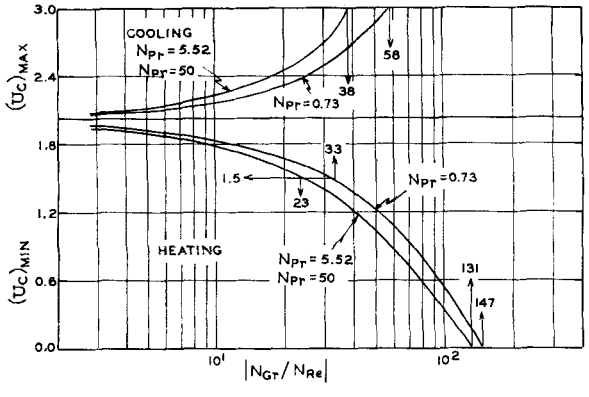

Fig. 6. Heating and cooling in upflow with variable density values of $(U_c)_{min}$ and $(U_c)_{max}$

Table 1. Heating in Upflow with Variable Density: Critical Values for Inversion and Flatness and Values of $(Z^*)_{lim}$ for Small Values of (N_{Gr}/N_{Re})

N_{Pr}	$(N_{Gr}/N_{Re})_{crit}$	$(Z^*)_{crit}\times 10^3$	$(N_{Gr}/N_{Re})_{flat}$	$(Z^*)_{m\text{-}flat}\times 10^3$	$(Z^*)_{lim}\times 10^3$
0.73	147	33	33	66	74
5.52	131	16	23	35	37
50	131	12	23	31	33

Table 2. Cooling in Upflow with Variable Density: Critical Values for Zero Velocity Gradient at the Wall and Values of $(Z^*)_{lim}$ for Small Values of $-(N_{Gr}/N_{Re})$

N_{Pr}	$-(N_{Gr}/N_{Re})^c{}_{crit}$	$(Z^*)^c{}_{crit}\times 10^3$	$(Z^*)_{lim}\times 10^3$
0.73	58	90	74
5.52	38	44	37
50	38	33	33

temperature is equal to 1, the values of the C's are not known since the temperature profile cannot be fitted to a step function. Therefore it is necessary to evaluate the dependent variables at a value other than $Z^* = 0$.

This may be done by use of the Leveque solution (*8*). Near the entrance of the tube where the thermal boundary layer is very thin and the amount of heating or cooling that has taken place is still very small, this theory should apply. The solution provides a means of evaluating q_w/A_t and T_m at any Z^* where the solution is valid. Knowing these quantities together with consistency conditions VIII, X, XI, and XV, one can determine the value of the constant K_3 and the five C's. Since q_w/A_t and T_m are functions only of Z^* and λ, the value of K_3, and the starting values of C can be determined once and for all at a given distance downstream for a given λ. The value of K_3, which was kept a constant downstream, can be thought of as providing a means of matching the fluxes for the approximate and Leveque solution at the selected value of Z^*. Farther downstream the consistency conditions and the over-all energy balance are used to carry out the integration. Two separate calculations were necessary, however, since the values for T_m and q_w/A_t from the constant-temperature-wall solution and the constant-ambient-temperature solution differ and the latter does not reduce to the former for $\lambda \to \infty$ $T_a \to 0$ except at $Z^* = 0$. The calculation for the finite wall-resistance case may be found in Rosen (*11*) as well as the procedure used for modifying the above for the small changes that take place in the velocity profile between the entrance and the Z^* selected to start the integration.

RESULTS OF THE APPROXIMATE SOLUTION

The ten simultaneous nonlinear differential equations were integrated numerically on the University of Illinois High Speed Digital Computer (ILLIAC). The results will be presented for the constant-temperature-wall case ($\lambda \to \infty$) at constant density and at constant viscosity, although the analysis applies to the simultaneous variation of both.

Heating in Upflow with Variable Density

At small values of N_{Gr}/N_{Re} the dimensionless center-line velocity will drop below 2 and after reaching a minimum will slowly return to 2 as the entire field becomes heated to the temperature of the wall. Figure 5 shows how the center-line velocity changes with Z^* for $N_{Gr}/N_{Re} = 100$ at $N_{Pr} = 5.52$, and Figure 6 shows the minimum center-line velocity reached, $(U_c)_{min}$, as a function of N_{Gr}/N_{Re}. It will be noted that the values for $N_{Pr} = 5.52$ and $N_{Pr} = 50$ fall on the same curve, though the values for $N_{Pr} = 0.73$ lie distinctly above. Figure 7 shows the location of the minimums in terms of Z^*.

The heating curves of Figure 6 may be extrapolated to $(U_c)_{min} = 0$ to find the value of $(N_{Gr}/N_{Re})_{crit}$. If the value of N_{Gr}/N_{Re} is greater than this number, then the center-line velocity will always drop to zero. The curves of Figure 7 may be extrapolated to these values of $(N_{Gr}/N_{Re})_{crit}$ to find the values of $(Z^*)_{crit}$ (Table 1). It would not be expected that inversion would take place at a Z^* greater than $(Z^*)_{crit}$.

The changes occurring in the velocity profile may be further characterized by the condition of flatness at the center of the tube defined by a zero value for $\left[\frac{\partial^2 U}{\partial R^2} + \frac{1}{R}\frac{\partial U}{\partial R}\right]_{R=0}$. The minimum value of N_{Gr}/N_{Re} which can cause the velocity profile to become flat can be read directly from Figure 6, since for the approximate velocity profile used in the analysis the profile is flat when $k_1 = 1.5$. These values of $(N_{Gr}/N_{Re})_{flat}$ are tabulated in Table 1 along with the $(Z^*)_{m\text{-}flat}$ associated with $(N_{Gr}/N_{Re})_{flat}$. Figure 8 indicates where the flat profile may be expected as a function of (N_{Gr}/N_{Re}).

It will be noted in Figure 7 that as $(N_{Gr}/N_{Re}) \to 0$ the values of $(Z^*)_{min}$ become constant. These values of $(Z^*)_{lim}$ which are listed in Table 1 give the value of Z^* at which the center-line velocity of flow profiles only slightly perturbed from the parabolic will reach a minimum in heating or a maximum in cooling.

Figure 9 is a plot of values of $(Z^*)_{null}$ (inversion points) for values of N_{Gr}/N_{Re} greater than the critical values. At $(N_{Gr}/N_{Re})_{crit}$ $(Z^*)_{min} =$

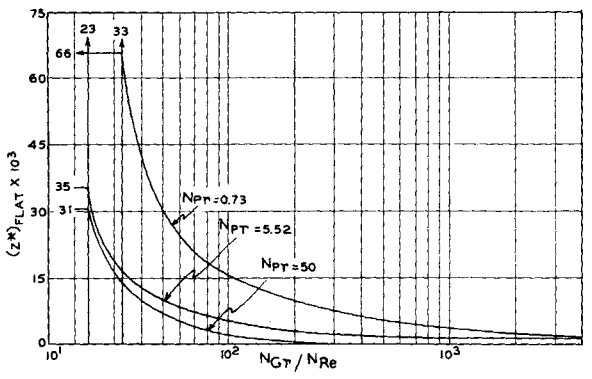

Fig. 8. Heating in upflow with variable density, values of $(Z^*)_{flat}$

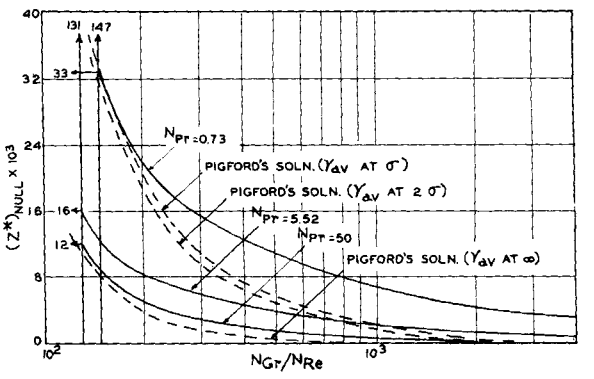

Fig. 9. Heating in upflow with variable density, values of $(Z^*)_{null}$

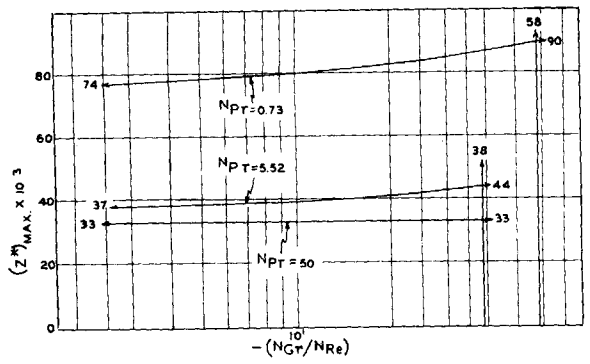

Fig. 10. Cooling in upflow with variable density, values of $(Z^*)_{max}$

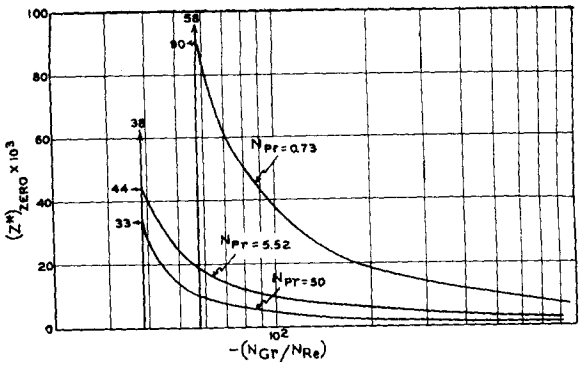

Fig. 11. Cooling in upflow with variable density, values of $(Z^*)_{zero}$

$(Z^*)_{null}$. Again the effect of N_{Pr} can be seen.

For comparison the values of $(Z^*)_{null}$ from the Pigford solution (see above) are plotted in Figure 9. Since the Pigford solution was derived for $N_{Pr} \to \infty$, it would be expected that the approximate solution curve for $N_{Pr} = 50$ could be compared with it. A large disagreement is noted however with γ_{avg} at 2 σ used. It will be shown later that the approximate solution predicts experimental inversion points satisfactorily, which would indicate that the Pigford solution is unsatisfactory for this purpose.

Cooling in Upflow with Variable Density

At small values of $-(N_{Gr}/N_{Re})$ the center-line velocity will rise above 2 and after reaching a maximum will slowly return to 2 as the entire fluid becomes cooled to the temperature of the wall. Figure 5 shows how the center-line velocity changes with Z^*, and on Figure 6 is plotted the maximum center-line velocity reached as a function of $-(N_{Gr}/N_{Re})$. As was the case for heating, the values for $N_{Pr} = 5.52$ and $N_{Pr} = 50$ fall on the same curve through the values for $N_{Pr} = 0.73$ lie distinctly below. Figure 10 shows the location of the maximums in terms of Z^*.

The cooling curves of Figure 6 may be extrapolated to $(U_c) = 3.0$, where the velocity gradient at the wall goes to zero for the velocity profile used in this study. If the curves of Figure 10 are extrapolated to these values of $-(N_{Gr}/N_{Re})^c{}_{crit}$, then the associated values of $(Z^*)^c{}_{crit}$ can be determined. It will be noted that as $-(N_{Gr}/N_{Re}) \to 0$, the value of $(Z^*)_{max} \to (Z^*)_{lim}$. These values are given in Table 2 and are the same as the values found for heating.

Figure 11 gives the location of the zero velocity gradient at the wall as a function of $-(N_{Gr}/N_{Re})$. The curves were extrapolated to the values of $(Z^*)^c{}_{crit}$, since at $(N_{Gr}/N_{Re})^c{}_{crit}$, $(Z^*)_{zero} = (Z^*)_{max}$.

Heating and Cooling in Upflow with Variable Viscosity

If ψ is positive (heating liquids), the center-line velocity decreases to a minimum greater than 1.5 and then increases slowly back to 2. If ψ is negative (cooling liquids), the center-line velocity increases to a maximum greater than 2 and then decreases back to 2. Figure 12 shows these effects.

The maximum and minimum center-line velocities reached for heating and cooling are plotted in Figure 13. The points for $N_{Pr} = 50$ fall on the same curve as the points for $N_{Pr} = 5.52$, although the points for $N_{Pr} = 0.73$ fall on a curve closer to the horizontal. Values of $(Z^*)_{max}$ and $(Z^*)_{min}$ are shown in Figure 14 as a function of μ_w/μ_o.

DISCUSSION OF RESULTS

The approximate solution may be checked by comparing it with an analytical solution which is available for fully developed flow in a tube with a constant flux wall, by examining the equations of motion and energy for very small values of $|N_{Gr}/N_{Re}|$, by comparing calculated inversion points with ones measured by experiment, and by comparing heat transfer coefficients at $N_{Gr}/N_{Re} = 0$ with the Graetz solution.

Deductions from the Fully Developed Constant Flux Solution

Heating in Upflow with Variable Density. Figure 6 shows how the minimum center-line velocity varies with N_{Gr}/N_{Re}. At the minimum, $(\partial U/\partial Z) = 0$ not only at the center but for the approximate profile used in this study also at every R. Whether or not $(\partial U/\partial Z) = 0$ at every R when $(\partial U/\partial Z) = 0$ at the center for real flows is not certain but is probably a fair approximation. A general analytical solution will be sought to the equations of motion and energy when this is the case.

The condition $(\partial U/\partial Z) = 0$ immediately leads to two results. First U must be a function of R alone, and second from Equation (1) V^* must be zero everywhere. If the following boundary-layer assumptions are made:

$$\frac{\partial p}{\partial r}, \frac{\partial^2 u}{\partial z^2}, \frac{\partial^2 t}{\partial z^2} = 0 \qquad (37)$$

then Equation (2), after division through by πN_{Pr}, becomes

$$0 = -N_{Re}\left(\frac{dP}{dZ}\right) - \frac{N_{Gr}}{N_{Re}}[T-1] + \frac{d^2U}{dR^2} + \frac{1}{R}\frac{dU}{dR} \qquad (38)$$

since T depends only on R at $(U_c)_{min\ or\ max}$. Taking $\nabla^2 = \frac{d^2}{dR^2} + \frac{1}{R}\frac{d}{dR}$ of both sides gives

$$0 = -\frac{N_{Gr}}{N_{Re}}\nabla^2 T + \nabla^4 U \qquad (39)$$

since the pressure drop is not a function of R. Dividing through by T_c results in

$$0 = -\frac{N_{Gr}}{N_{Re}}\nabla^2\left(\frac{T}{T_c}\right) + \nabla^4\left(\frac{U}{T_c}\right) \qquad (40)$$

Equation (3) becomes

$$U\frac{\partial T}{\partial Z} = \frac{1}{N_{Re}N_{Pr}}\nabla^2 T \qquad (41)$$

or dividing by T_c gives

$$U\frac{\partial t}{\partial Z} = \frac{t_c - t_w}{N_{Re}N_{Pr}}\nabla^2\left(\frac{T}{T_c}\right) \qquad (42)$$

Substitution of Equation (40) into Equation (42) results in

$$U\frac{\partial t}{\partial Z} = \frac{t_c - t_w}{N_{Re}N_{Pr}}\left[\frac{N_{Re}}{N_{Gr}T_c}\nabla^4 U\right] \qquad (43)$$

Since the right-hand side of Equation (43) is a function of R alone,

$$\frac{\partial t}{\partial Z} = A \text{ (a constant)} \qquad (44)$$

Letting

$$K = \frac{AN_{Gr}\,N_{Pr}\,T_c}{(t_c - t_w)} \qquad (45)$$

one gets for heating

$$\nabla^4 U + KU = 0 \qquad (46)$$

Equations (42) and (46) arise in the analysis of fully developed constant-flux heating in upflow and have been solved by Hanratty, Rosen, and Kabel (5) and by Hallman (4). The solutions for the temperature and velocity fields are unique functions of $N_{Gr}\,T_c/N_{Re}$.

Figure 15 compares the values of $(U_c)_{min}$ vs. $(N_{Gr}/N_{Re})\,(T_c)_{min}$ from the approximate solution to the analytical solution. It can be seen that multiplying N_{Gr}/N_{Re} by $(T_c)_{min}$ brings the values at the different N_{Pr} together. The analytical solution gives $(N_{Gr}T_c/N_{Re})_{flat} = 22$ and $(N_{Gr}T_c/N_{Re})_{crit} = 121.6$, which are in good agreement with the approximate solution results. Figures 16 and 17 compare the analytical and approximate velocity and temperature profiles at the Z^* at which U_c is a minimum.

Cooling in Upflow with Variable Density. The analysis for cooling in upflow when $\psi = 0$ is the same as for heating in upflow with variable density except that Equation (46) becomes

$$\nabla^4 U - KU = 0 \qquad (47)$$

The solution of Equations (42) and (45) is also given in references 4 and 5. The temperature and velocity fields are a unique function of $-N_{Gr}\,T_c/N_{Re}$.

Figure 15 compares the values of $(U_c)_{max}$ *vs.* $(N_{Gr}/N_{Re})\,(T_c)_{max}$ taken from the approximate solution to the analytical solution. Multiplying $-N_{Gr}/N_{Re}$ by $(T_c)_{max}$ again brings the values for the different N_{Pr} together. The analytical solution gives $-N_{Gr}\,T_c/N_{Re} = 49.2$ as the critical for causing the velocity gradient at the wall to go to zero compared with the approximate solution value of about 38. The center-line velocity is 3.2 according to the analytical solution at this point but is only 3.0 according to the approximate solution. The temperature and velocity fields at the maximum center-line velocity where $-N_{Gr}/N_{Re}\,(T_c)_{max} = 25.1$ are compared with the analytical solution in Figures 16 and 17.

Heating and Cooling in Upflow with Variable Viscosity

The general trends of Figure 13 can probably best be understood by recourse to certain qualitative arguments. When $N_{Pr} \to 0$ the thermal boundary layer builds up so fast that the fluid becomes isothermal almost immediately and there is no change in center-line velocity. Therefore the straight line at $k_1 = 2.0$ is a limiting solution for very small Pr.

At high Pr the thermal boundary layer builds up very slowly, and for large ψ (heating) the large velocity gradient at the wall due to the small viscosity would cause the profile to flatten out toward plug type of flow. This trend can be seen in Figure 13 for the high Pr curve, which approaches $k_1 = 1.5$ as ψ becomes very large. True plug flow would have the velocity everywhere equal to 1, but the flattest that the approximate profile can get is when $k_1 = 1.5$ ($k_2 = 0$).

At intermediate values of N_{Pr} the two effects compete. The flattening caused by the small viscosity ratio (large ψ) is compensated by the growing thermal boundary layer, and so even when ψ becomes very large a plug type of profile is not achieved. This is demonstrated by the $N_{Pr} = 0.73$ curve.

The situation for cooling is somewhat different. As $\psi \to -1$, the flow at the wall is greatly decelerated, which forces the center-line velocity to increase sufficiently to compensate. This causes the center-line velocity to go to very large values in the limit as $\psi \to -1$, as is suggested by the curve for $N_{Pr} = 5.52$ and 50.

Behavior at Small $|N_{Gr}/N_{Re}|$

Figures 7 and 8 show that the values of $(Z^*)_{min}$ and $(Z^*)_{max}$ approach limiting values at small values of $|N_{Gr}/N_{Re}|$. Those values of $(Z^*)_{lim}$ which are a function of N_{Pr} alone are listed in Tables 1 and 2. The behavior of $(Z^*)_{min}$ and $(Z^*)_{max}$ at small $|N_{Gr}/N_{Re}|$ can be deduced directly from an examination of the equations of energy and motion.

For a constant-temperature wall Equation (2) becomes

$$V^* \frac{\partial U}{\partial R} + U \frac{\partial U}{\partial Z^*} = -\frac{dP}{dZ^*} - \pi N_{Pr} \left| \frac{N_{Gr}}{N_{Re}} \right| [T - 1] + \pi N_{Pr} \left[\frac{\partial^2 U}{\partial R^2} + \frac{1}{R}\frac{\partial U}{\partial R} \right] \qquad (48)$$

At small $|N_{Gr}/N_{Re}|$ the flow field is only slightly perturbed from the Graetz solution and the variables may be written as

$$V^* = V' \text{ (since } V_g = 0)$$
$$U = U_g + U'$$
$$T = T_g + T'$$
$$P = P_g + P' \qquad (49)$$

Substituting these quantities into Equation (48), neglecting T' compared with T_g, and dropping second-order perturbation terms as small, one obtains

$$V' \frac{\partial U_g}{\partial R} + U_g \frac{\partial U'}{\partial Z^*} = -\frac{dP'}{dZ^*} - \pi N_{Pr} \left| \frac{N_{Gr}}{N_{Re}} \right| (T_g - 1) + \pi N_{Pr} \left[\frac{\partial^2 U'}{\partial R^2} + \frac{1}{R}\frac{\partial U'}{\partial R} \right] \qquad (50)$$

since

$$\frac{dP_g}{dZ^*} = \pi N_{Pr} \left[\frac{\partial^2 U_g}{\partial R^2} + \frac{1}{R}\frac{\partial U_g}{\partial R} \right] \qquad (51)$$

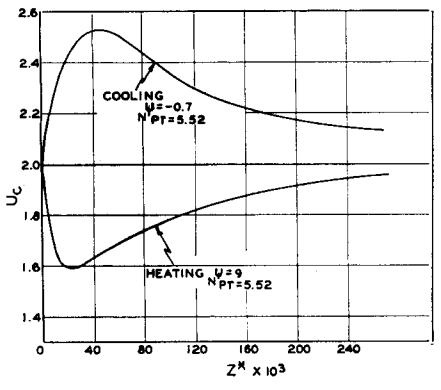

Fig. 12. Heating and cooling in upflow with variable viscosity, changes in center-line velocity as a function of Z*.

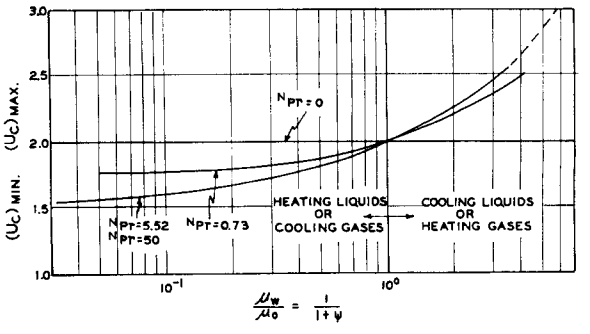

Fig. 13. Heating and cooling in upflow with variable viscosity, values of $(U_c)_{min}$ and $(U_c)_{max}$

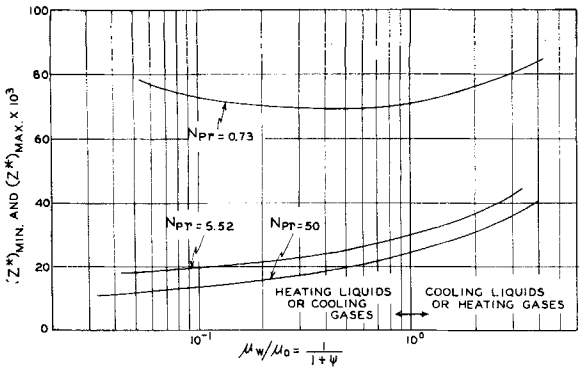

Fig. 14. Heating and cooling in upflow with variable viscosity, values of $(Z^*)_{min}$ and $(Z^*)_{max}$

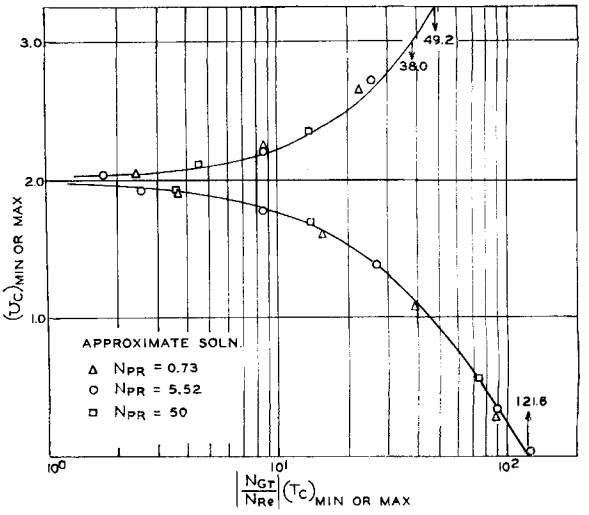

Fig. 15. Comparison of the approximate and analytical solution, center-line velocities for cooling and heating in upflow.

Equation (3) becomes on substitution

$$U_g \frac{\partial T_g}{\partial Z^*} = \pi \left[\frac{\partial^2 T_g}{\partial R^2} + \frac{1}{R} \frac{\partial T_g}{\partial R} \right] \quad (52)$$

since the V' and U' terms are small.

If

$$U'^* = \frac{U'}{|N_{Gr}/N_{Re}|} \quad (53)$$

Equation (50) becomes

$$V' \frac{\partial U_g}{\partial R} + \left| \frac{N_{Gr}}{N_{Re}} \right| U_g \frac{\partial U'^*}{\partial Z^*} = -\frac{dP'}{dZ^*} - \pi N_{Pr} \left| \frac{N_{Gr}}{N_{Re}} \right| [T_g - 1] + \pi N_{Pr} \left| \frac{N_{Gr}}{N_{Re}} \right| \left[\frac{\partial^2 U'^*}{\partial R^2} + \frac{1}{R} \frac{\partial U'^*}{\partial R} \right] \quad (54)$$

From Equation (1) it may be noted that

$$V' = -\left| \frac{N_{Gr}}{N_{Re}} \right| \frac{1}{R} \int_0^R R \frac{\partial U'^*}{\partial Z^*} dR \quad (55)$$

If now dP'/dZ^* is deduced from Equation (10) or (12), then every term in Equation (54) has a $|N_{Gr}/N_{Re}|$ term in it which cancels out, with the result that

$$U'^* = f_1 (R, Z^*, T_g, N_{Pr}) \quad (56)$$

But from Equation (52)

$$T_g = f_2 (R, Z^*) \quad (57)$$

therefore

$$U_1'^* = f_3 (R, Z^*, N_{Pr}) \quad (58)$$

or

$$U' = \left| \frac{N_{Gr}}{N_{Re}} \right| f_3 (R, Z^*, N_{Pr}) \quad (59)$$

and

$$U = U_g + \left| \frac{N_{Gr}}{N_{Re}} \right| f_3 (R, Z^*, N_{Pr}) \quad (60)$$

Equation (60) would describe the velocity field as a function of R, Z^*, and N_{Pr} if the function f_3 (R, Z^*, N_{Pr}) were known. In order to find the value of $(Z^*)_{min}$ or $(Z^*)_{max}$ as $|N_{Gr}/N_{Re}| \to 0$, Equation (60) should be differentiated with respect to Z^* and then the derivative set equal to zero:

$$\frac{\partial U_c}{\partial Z^*} = 0 = f_3' [(Z^*)_{lim}, N_{Pr}]_{R=0} \quad (61)$$

The function on the right can be solved for $(Z^*)_{lim}$ in terms of N_{Pr} alone; that is

$$(Z^*)_{lim} = f_4 (N_{Pr}) \quad (62)$$

This analysis is valid for both heating and cooling, so that $(Z^*)_{lim}$ should be the same for heating and for cooling as was found in the approximate solution.

Comparison to Experiment

Heating in Upflow. Experiments conducted with water in a vertical tube with a calming section and a constant outside wall temperature have been described previously (*5, 11, 12*). When the flow field was flooded with dye and N_{Gr}/N_{Re} was above the critical, a long cigar-shaped paraboloid was observed to form and the apex of this paraboloid was taken to be the point where the center-line velocity dropped to zero. In order to compare these experimental observations with the approximate solution, several runs were made on ILLIAC with parameters corresponding to the experimental conditions, and the point at which the center-line velocity became zero was calculated. Although there was a small variation in ψ and N_{Pr} in the experimental data, all the data were plotted together in Figure 18 for comparison with the ILLIAC results calculated from the average experimental values for ψ $(=0.3)$ and N_{Pr} $(=6.0)$. The agreement between experiment and the approximate solution is satisfactory when the inversion point is far downstream. However when $N_{Gr}/N_{Re} \gtrsim 500$ [based on $(t_a - t_0)$] and the inversion point is very close to the start of the heat transfer section, agreement is rather poor. This may be due to two reasons. The first is that at large N_{Gr}/N_{Re} the conditions near the entrance are changing so fast that the boundary-layer assumptions may no longer be valid. The second reason is that there is a real doubt as to how closely the experimental conditions approximated a step rise in temperature. Failure to achieve a step rise would cause the paraboloid to appear farther downstream. This is, in fact, what Figure 18 indicates.

Cooling in Upflow. Below $-N_{Gr}/N_{Re}$ of about 70 (based on $t_a - t_0$) dye injected into the center of the tube would flow out the top of the tube without being disturbed. At larger values of $-N_{Gr}/N_{Re}$ the dye would move off center owing to the formation of an asymmetric region of downflow in a portion of the tube, and, depending on the value of N_{Re} as $-N_{Gr}/N_{Re}$ was increased, the dye filament would break up. Further increase in $-N_{Gr}/N_{Re}$ caused the point of breakup to

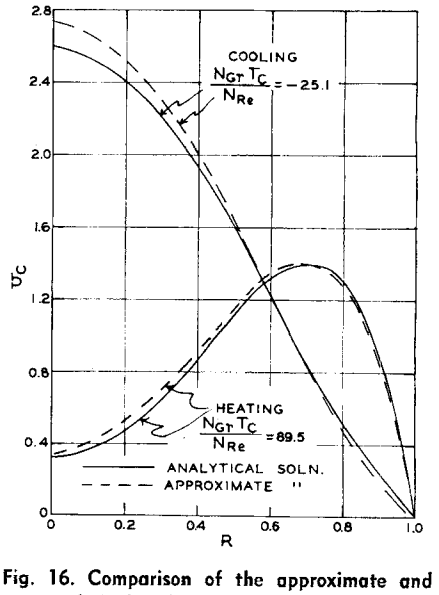

Fig. 16. Comparison of the approximate and analytical solution velocity profiles.

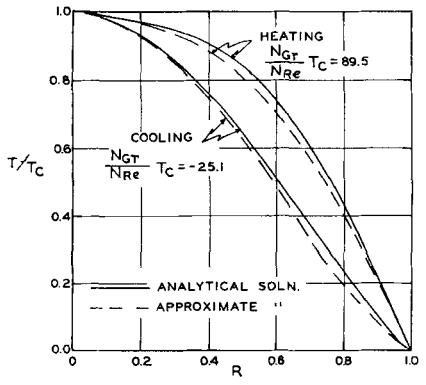

Fig. 17. Comparison of the approximate and analytical solution temperature profiles.

move upstream until the dye would break up almost immediately upon entering the heat transfer section.

In order to compare these observations with the approximate solution, several runs were made on ILLIAC to calculate the point at which the velocity gradient at the wall went to zero. In general the breakup points appeared to occur downstream of the point where the velocity gradient was calculated to go to zero. This would imply that reversal of flow at the wall is possible before the field breaks down into turbulence, and the visual observations tended to confirm this (*12*).

Heat Transfer Coefficients

Although the approximate solution appears to predict satisfactorily the general nature of the flow field over the whole range of Gz when $|N_{Gr}/N_{Re}|$ is less than the critical values, and at least up to the point of inversion for heating when N_{Gr}/N_{Re} is greater than the critical but less than about 500, the solution appears to give poor (in general low) heat transfer coefficients. This is due to the fact that heat transfer coefficients are highly dependent on the slope of the velocity profile at the wall and the simple three coefficient velocity profile used in the approximate solution could not satisfactorily predict these slopes. Local and average heat transfer coefficients (see notation) of the approximate solution are compared with the Graetz solution as given by Sellars, Tribus, and Klein (*15*) ($N_{Gr}/N_{Re} = O$ and $\psi = O$) and the limiting Leveque solution in Figure 19. Local heat transfer coefficients occurring at the point of the maximum and the minimum center-line velocity are compared with the analytical solution of Equations (42), (46), and (47) in Figures 20 and 21.

To calculate heat transfer coefficients Pigford (*10*) employed the same approach as Martinelli and Boelter (*2, 8*) using a semitheoretical expression of the same form as the Leveque solution. This expression and his results for N_{Nu_m} and T_m are given in the notation. From the form of the equation for N_{Nu_m} it can be seen that the Pigford solution does not approach an asymptote at low values of N_{Gz} as the Graetz solution predicts. (See also *4.*)

For situations in which natural convection is negligible the correlation of Sieder and Tate (*16*) has been widely used. (See notation.) Figure 22 compares this correlation with the approximate solution as well as with the Pigford solution (shown for heating only). It can be seen that the approximate solution is very low for heating, though the Pigford solution shows good agreement. For cooling, the approximate solution appears to show better agreement.

Good experimental heat transfer data for situations in which natural convection is important but viscosity variation can be neglected do not appear to be available in the literature, and the theory cannot be directly compared with experiment. However it is of interest to discuss Pigford's solution for this case. Figure 23 is a plot of average Nusselt number (N_{Nu_a}) vs. N_{Gz} with N_{Gr}/N_{Re} as parameter. [Martinelli and Boelter (*8*) and Pigford (*10*) used $N_{Gr}N_{Pr}/Z$ as a parameter.] From the approximate-solution results presented for the velocity field a line of inversion may be constructed (the $N_{Pr} = 50$ results). It tangentially meets the $(N_{Gr}/N_{Re})_{crit} = 131$ line at $(Z^*)_{crit}$. (See Table 1.) The area upward and to the left of this line represents an area where inversion takes place with turbulence appearing downstream. Agreement between experiment and the theory based on a laminar-flow model should not be expected in this region.

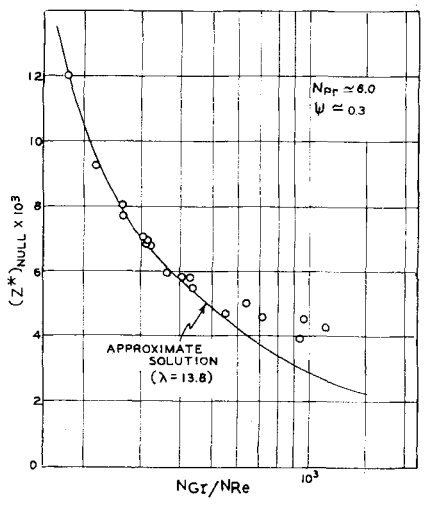

Fig. 18. Comparison of experimental inversion points and the approximate theory.

ACKNOWLEDGMENT

This work was initiated by a grant from Research Corporation, and funds from the Office of Ordnance Research under Project 1256 Contract DA-11-022-ORD-1707 were also made available. This aid is gratefully acknowledged.

NOTATION

a = inside radius of tube, ft.

A = parameter arising in fully developed constant flux solution, defined by Equation (44), °F.

A_i = inside area of tube, sq. ft.

b = temperature coefficient of viscosity, °F.$^{-1}$

c_p = heat capacity at constant pressure, B.t.u./(lb.$_m$) (°F.)

$C_1 \ldots C_5$ = coefficients of the temperature profile series—a function of Z^* alone, dimensionless

d = outside radius of the tube, ft.

$f_1(x) \ldots f_4(x)$ = functions of the variables indicated in Equations (56), (57), (58), and (62), dimensionless

g = acceleration of gravity equal to 4.17 x 10^8 ft./hr.^{2}

g_c = conversion factor equal to 4.17 x 10^8 (lb.-mass) (ft.)/(hr.^{2}) (lb.-force)

h_a = average heat transfer coefficient based on the average of the differences between the ambient and mean temperature at the inlet and outlet, B.t.u./(hr.) (sq. ft.) (°F.)

h_m = local heat transfer coefficient based on local wall minus local mean temperature, B.t.u./(hr.) (sq. ft.) (°F.)

h_o = local heat transfer coefficient based on local wall minus entrance temperature, B.t.u./(hr.) (sq. ft.) (°F.)

$I_1(\sigma), I_3(\sigma)$ = integrals defined by Equations (19) and (20) respectively, dimensionless

$I_5(R,\sigma), I_7(R,\sigma)$ = integrals defined by Equations (21) and (29) respectively, dimensionless

k, k_s = thermal conductivity of the fluid and wall, respectively, B.t.u./(hr.) (ft.) (°F.)

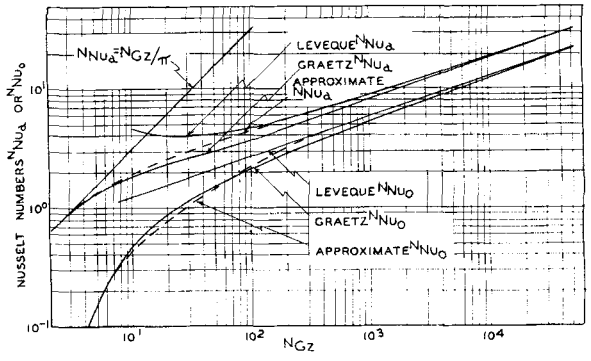

Fig. 19. Comparison of the approximate and Graetz and Leveque solution, Nusselt numbers N_{Nu_a} and N_{Nu_o}.

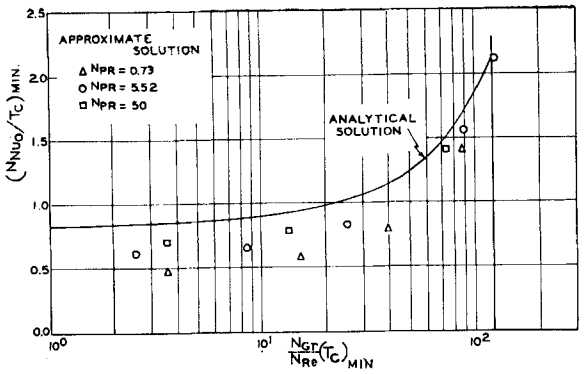

Fig. 20. Comparison of the approximate and analytical solution, Nusselt numbers for heating in upflow.

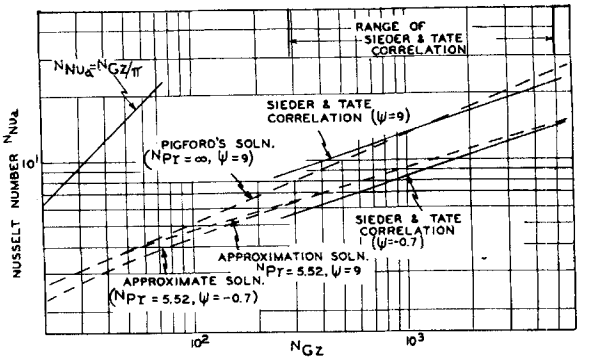

Fig. 22. Comparison of average Nusselt numbers N_{Nu_a} for heating and cooling in upflow with variable viscosity.

k_1, k_2, k_3 = coefficients of the approximate velocity profile series, a function of Z^* alone, dimensionless

K = parameter arising in the fully developed constant flux solution defined by Equation (45), dimensionless

K_3 = constant arising in the approximate solution used to fit the approximate solution to the Leveque solution, dimensionless

N_{Gr} = Grashof number equal to $a^3\rho_o^2 g \beta_o (t_d - t_o)/\mu_o^2$, dimensionless; when the wall temperature is constant $t_d \rightarrow t_w$

$(N_{Gr}/N_{Re})_{crit}$ = minimum (N_{Gr}/N_{Re}) needed in heating in upflow to cause inversion, dimensionless

$(N_{Gr}/N_{Re})_{flat}$ = minimum (N_{Gr}/N_{Re}) needed in heating upflow to cause the velocity profile at the center to become flat, dimensionless

$(N_{Gr}/N_{Re})^o_{crit}$ = minimum (N_{Gr}/N_{Re}) needed in cooling in upflow to cause the velocity gradient at the wall to go to zero, dimensionless

N_{Gz} = Graetz number equal to $(\pi N_{Re} N_{Pr})/Z$

N_{Nu_a} = average Nusselt number equal to

$$\frac{h_a a}{k} = \frac{N_{Gz}}{\pi}\left[\frac{1 - T_m}{1 + T_m - 2T_d}\right]$$

dimensionless

N_{Nu_m} = local Nusselt number equal to $\frac{h_m a}{k} = -\frac{1}{T_m}\left[\frac{\partial T}{\partial R}\right]_{R=1}$, dimensionless

N_{Nu_o} = local Nusselt number equal to $\frac{h_o a}{k} = -\left[\frac{\partial T}{\partial R}\right]_{R=1}$, dimensionless

$N_{(Nu_o)_{max}}$ = value of the local Nusselt number at $(U_c)_{max}$, dimensionless

$N_{(Nu_o)_{min}}$ = value of the local Nusselt number at $(U_c)_{min}$ dimensionless

N_{Nu_o}/T_c = Nusselt number arising in the fully developed constant flux solution equal to $-q_w a/A_i\ k(t_c - t_w)$, dimensionless

N_{Pr} = Prandtl number equal to $c_p\mu_o/k$, dimensionless

N_{Re} = Reynolds number equal to $aU_{avg}\rho_o/\mu_o$, dimensionless

o = subscript to denote entrance conditions

p = pressure, lb.-force/sq. ft.

P = pressure equal to $(g_c p + \rho_o g z)/\rho_o U^2_{avg}$, dimensionless

q_w = heat flow at the wall, B.t.u./hr.

r = distance measured from center of tube out radially, ft.

R = number of tube radii equal to r/a, dimensionless

t = temperature at any point, °F.

t_c = temperature at the center of the tube, °F.

t_d = jacket or ambient temperature, °F.

t_m = mean or mixing-cup temperature, °F.

t_w = temperature of the wall or inside of the tube, °F.

T = temperature equal to $T_A T_c = (t - t_w)/(t_c - t_w)$, dimensionless

T_A = temperature equal to $(t - t_w)/(t_c - t_w)$, dimensionless

T_c = temperature equal to $(t_c - t_w)/(t_o - t_w)$, dimensionless

T_d = temperature equal to $(t_d - t_w)/(t_o - t_w)$, dimensionless

T_g = temperature from the Graetz solution, dimensionless

T' = perturbation on the Graetz solution temperature, dimensionless

T_m = temperature defined by Equation (13) equal to $(t_m - t_w)/(t_o - t_w)$, dimensionless

T_{av} = temperature defined by

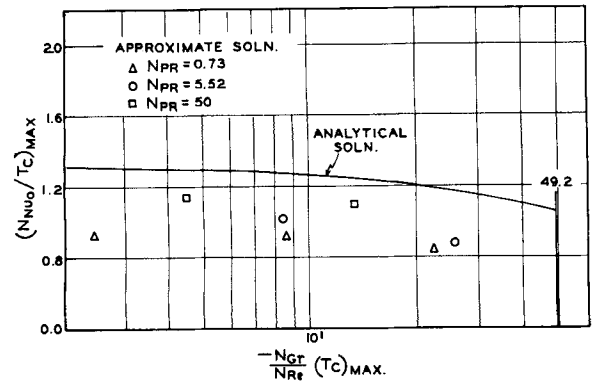

Fig. 21. Comparison of the approximate and analytical solution, Nusselt numbers for cooling in upflow.

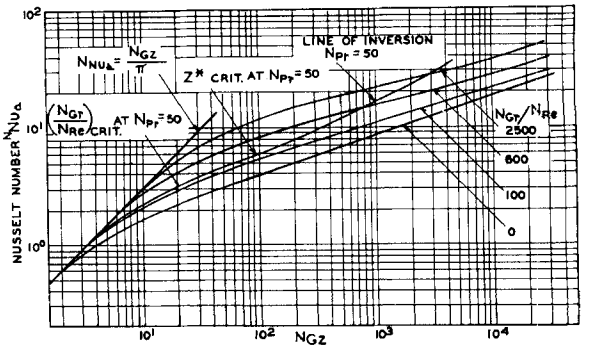

Fig. 23. Values of N_{Nu_a} according to the solution of Pigford for heating in upflow with variable density ($N_{Pr} = \infty$, γ_{avg} evaluated at 2 σ)

Equation (14), dimensionless

$(T_c)_{max}$ = value of T_c at $(U_c)_{max}$

$(T_c)_{min}$ = value of T_c at $(U_c)_{min}$

u = local velocity in the z direction, ft./hr.

U = u/U_{avg}, dimensionless

U' = perturbation on the Graetz solution velocity in the Z direction, dimensionless

U'^* = defined by Equation (53), dimensionless

U_{avg} = average velocity in the Z direction, ft./hr.

U_c = center-line velocity, dimensionless; subscripts min and max refer to the minimum and maximum center-line velocity reached

U_g = velocity in the Z direction from the Graetz solution, dimensionless

v = local velocity in the r direction, ft./hr.

V = equal to v/U_{avg}, dimensionless

V^* = equal to $\pi N_{Re} N_{Pr} V$, dimensionless

V' = perturbation to the Graetz solution velocity in the r direction, dimensionless

w = dummy variable defined by Equation (24), dimensionless

z = distance measured downstream from the start of the heat transfer section, ft.

Z = number of tube radii downstream measured from the start of the heat transfer section equal to z/a, dimensionless

Z^* = $1/N_{Gz} = Z/\pi N_{Re} N_{Pr}$, dimensionless

$(Z^*)_{crit}$ = location at which inversion takes place when N_{Gr}/N_{Re} is equal to the critical value for heating in upflow, dimensionless

$(Z^*)_{flat}$ = location at which the velocity profile first becomes flat during heating in upflow, dimensionless

$(Z^*)_{lim}$ = location at which the center-line velocity reaches a minimum or maximum for heating or cooling in upflow as $|N_{Gr}/N_{Re}| \to 0$, dimensionless

$(Z^*)_{m\text{-}flat}$ = location at which the velocity profile at the center becomes flat when N_{Gr}/N_{Re} is equal to $(N_{Gr}/N_{Re})_{flat}$, dimensionless

$(Z^*)_{max}$ = location at which the center-line velocity reaches its maximum during cooling in upflow, dimensionless

$(Z^*)_{min}$ = location at which the center-line velocity reaches its minimum during heating in upflow, dimensionless

$(Z^*)_{null}$ = location at which inversion takes place, dimensionless

$(Z^*)_{zero}$ = location at which the velocity gradient at the wall goes to zero, dimensionless

$(Z^*)^c_{crit}$ = location at which the velocity gradient goes to zero when (N_{Gr}/N_{Re}) is equal to $(N_{Gr}/N_{Re})^c_{crit}$, dimensionless

$$T_m = \frac{4(3)^{1/3}\gamma_{avg}}{e^{\Gamma\left(\frac{4}{3}\right)\sigma^{2/3}}}$$

$$N_{Nu_m} = \frac{1}{\Gamma(4/3)}\left(\frac{\sigma}{9}\right)^{1/3}$$

Sieder-Tate Equation

$$N_{Gz} = \left[\frac{0.93\,\pi\left(\frac{4}{\pi}\right)^{1/3}\left[1+\frac{\psi}{2}(T_m+1)\right]^{0.14}}{\left(\frac{1-T_m}{1+T_m}\right)}\right]^{3/2}$$

Greek Letters

β = coefficient of cubical expansion, °F.$^{-1}$

γ = ratio of actual velocity gradient at the wall to the velocity gradient of a parabola, dimensionless

γ_{avg} = average ratio of the actual velocity gradient at the wall to the velocity gradient of a parabola, dimensionless

$\Gamma(x)$ = gamma function

λ = system parameter equal to $k_s/[k \ln(d/a)]$, dimensionless

μ = viscosity of the fluid, lb.-mass (ft.) (hr.)

μ_b = viscosity of the fluid evaluated at the bulk temperature or average of the inlet and outlet mean temperatures, lb.-mass/(ft.)(hr.)

μ_o = viscosity of fluid evaluated at the entrance temperature, lb.-mass/(ft.)(hr.)

μ_w = viscosity of fluid evaluated at the wall temperature, lb.-mass/(ft.)(hr.)

π = constant equal to 3.14159265

ρ = density of fluid, lb.-mass/cu. ft.

ρ_o = density of fluid evaluated at entrance temperature, lb.-mass/cu. ft.

σ = $(4\,\gamma_{avg} N_{Gz})/\pi$, dimensionless

ψ = system parameter equal to $b(t_a - t_o)$, $b(t_w - t_o)$ for a constant temperature wall and $(\mu_o/\mu_w) - 1$, dimensionless

$$\nabla^2(x) = \left(\frac{d}{dr^2} + \frac{1}{r}\frac{d}{dr}\right)(x)$$

$$\nabla^4(x) = \left(\frac{d}{dr^2} + \frac{1}{r}\frac{d}{dr}\right)\left(\frac{d}{dr^2} + \frac{1}{r}\frac{d}{dr}\right)(x)$$

Pigford Solution

$$q_w/A_t = \frac{k(t_w - t_m)}{a\,\Gamma(4/3)}\left(\frac{\sigma}{9}\right)^{1/3}$$

LITERATURE CITED

1. Acrivos, Andreas, *A.I.Ch.E. Journal*, 4, 285 (1958).
2. Boelter, L. M. K., V. H. Cherry, H. A. Johnson, and R. C. Martinelli, "Heat Transfer Notes," X-19, University of California Press, Berkeley (1948).
3. Eckert, E. R. G., and A. J. Diaguila, *Trans. Am. Soc. Mech. Engrs.*, **76**, 497 (1954).
4. Hallman, T. M., *ibid.*, **78**, 1831 (1956); Ph.D. thesis, Purdue University, Lafayette, Indiana (1958).
5. Hanratty, T. J., E. M. Rosen, and R. L. Kabel, *Ind. Eng. Chem.*, **50**, 815 (1958).
6. Keevil, C. S., and W. H. McAdams, *Chem. Met. Eng.*, 36, 464 (1929).
7. Lee, A., W. O. Nelson, V. H. Cherry, and L. M. K. Boelter, "Proceedings of the Fifth International Congress of Applied Mechanics," Wiley, New York (1939).
8. Martinelli, R. C., and L.M.K. Boelter, "The Analytical Prediction of Superposed Free and Forced Viscous Convection in a Vertical Pipe," Vol. 5, p. 23. University of California Publications in Engineering, Berkeley (1942).
9. Millsaps, K., and K. Pohlhausen, "Proceedings of the Conference on Differential Equations," Univ., Maryland, College Park (1955).
10. Pigford, R. L., *Chem. Eng. Progr. Symposium Ser. No. 17*, **51**, 79 (1953).
11. Rosen, E. M., Ph.D. thesis, Univ. of Ill., Urbana (1959).
12. Scheele, G. F., E. M. Rosen, and T. J. Hanratty, *Can. J. Chem. Eng.*, 38, 67 (1960).
13. Schenk, J., and J. M. Dumore, *Appl. Sci. Res.*, **A4**, 39 (1953).
14. Schlichting, Hermann, "Boundary Layer Theory," pp. 94, 201, 204, McGraw-Hill, New York (1955).
15. Sellars, J. R., M. Tribus, and J. S. Klein, *Trans. Am. Soc. Mech. Engrs.*, 78, 441 (1956).
16. Sieder, E. N., and G. E. Tate, *Ind. Eng. Chem.*, 28, 1429 (1936).
17. Singh, S. N., *Appl. Sci. Res.*, A7, 325 (1958).
18. Whiteman, I. R., and W. B. Drake, *Am. Soc. Mech. Engrs.*, 38, 728 (1958).
19. Yamagata, K., *Fac. Eng., Kyushu Imperial Univ.*, 7, 366 (1940).

Manuscript received November 10, 1959; revision received May 10, 1960; paper accepted May 11, 1960.